eNeuro

Research Article: New Research | Cognition and Behavior

Encoding of the Intent to Drink Alcohol by the Prefrontal Cortex is blunted in Rats with a Family History of Excessive Drinking

https://doi.org/10.1523/ENEURO.0489-18.2019

Cite as: eNeuro 2019; 10.1523/ENEURO.0489-18.2019

Received: 13 December 2018
Revised: 19 April 2019
Accepted: 1 June 2019

1. Title: Encoding of the Intent to Drink Alcohol by the Prefrontal Cortex is blunted in Rats with a Family History of Excessive Drinking

2. Abbreviated Title: Neural Encoding of the Intention to Drink Alcohol

3. Author Names and Affiliations: David N. Linsenbardt*, Nicholas M. Timme, & Christopher C. Lapish

Addiction Neuroscience, Department of Psychology and Indiana Alcohol Research Center, Indiana University – Purdue University Indianapolis, Indianapolis, IN 46202

4. Author contributions: DNL and CCL designed research, DNL performed research, and DNL, CCL, and NMT analyzed data and wrote the paper.

5. Correspondence address:
David N. Linsenbardt*, PhD
Addiction Neuroscience
Department of Psychology
Indiana University - Purdue University Indianapolis
402 N Blackford St, LD 124
Indianapolis, IN 46202
Phone: 317-721-6092
Fax: 317-274-6756
Email: dlinsenb@iupui.edu

6. Number Figures: 6

7. Number Tables: 1

8. Number Multimedia: 4

9. Number words for Abstract: 181

10. Number words for Significance Statement: 120

11. Number words for Introduction: 640

12. Number words for Discussion: 981

13. Acknowledgements: This research was supported in part by Lilly Endowment, Inc., through its support for the Indiana University Pervasive Technology Institute, and in part by the Indiana METACyt Initiative. The Indiana METACyt Initiative at IU is also supported in part by Lilly Endowment, Inc.

14. Conflicts of Interest: None

15. Funding Sources: This work was supported by NIAAA grant #'s AA022268 (DNL), AA025120 (DNL), AA007462 (NMT), AA022821 (CCL), AA023786 (CCL), the ABMRF (CCL), and the Indiana Alcohol Research Center P60AA007611 (D. Kareken).

The prefrontal cortex plays a central role in guiding decision-making, and its function is altered by alcohol use and an individual's innate risk for excessive alcohol drinking. The primary goal of this work was to determine how neural activity in the prefrontal cortex guides the decision to drink. Towards this goal, the within-session changes in neural activity were measured from medial prefrontal cortex (mPFC) of rats performing a drinking procedure that allowed them to consume or abstain from alcohol in a self-paced manner. Recordings were obtained from rats that either lacked or expressed an innate risk for excessive alcohol intake - Wistar or Alcohol Preferring 'P' rats, respectively. Wistar rats exhibited patterns of neural activity consistent with the intention to drink or abstain from drinking, whereas these patterns were blunted or absent in P rats. Collectively, these data indicate that neural activity patterns in mPFC associated with the intention to drink alcohol are influenced by innate risk for excessive alcohol drinking. This observation may indicate a lack of control over the decision to drink by this otherwise well-validated supervisory brain region.

Key Words: alcohol-associated cues; alcohol-preferring rat; prefrontal cortex; electrophysiology; neural encoding; information theory; decision-making

64 Aberrant decision-making is both a risk factor for, and the result of, an Alcohol
65 Use Disorder (AUD; (Verdejo-Garcia et al., 2017). Therefore, understanding the neural
66 systems that underlie decision-making, and how altered function of these systems
67 influences decisions about drinking alcohol, is critical to identify novel targets to treat
68 and prevent AUDs. While several neural systems have been implicated in decision-
69 making, the medial prefrontal cortex (mPFC) plays a critical role in setting goals
70 (Buschman and Miller, 2014) and forming intentions to achieve them (Fuster and
71 Bressler, 2015, Brass et al., 2013, Haynes et al., 2007). Thus, the inability to refrain
72 from excessive drinking may reflect pathology in neural circuits that guide goal-directed
73 actions such as mPFC (Fuster and Bressler, 2015).
74 Dysfunction of the mPFC has been repeatedly found in populations of subjects
75 that drink alcohol excessively (Schacht et al., 2013). Exposure to experience- or
76 experimentally-paired alcohol cues, increases neuronal activity within the PFC (Tapert
77 et al., 2003, George et al., 2001, Kareken et al., 2010), and the magnitude of this effect
78 is correlated with increases in self-reported alcohol craving (Myrick et al., 2004) and
79 relapse (Grusser et al., 2004). Additionally, recently abstinent individuals with an AUD
80 exhibit reduced baseline neuronal activity within the mPFC (Catafau et al., 1999).
81 Similar effects are observed in rodents, with exposure to alcohol-associated cues
82 eliciting reinstatement of extinguished alcohol seeking and robust increases in
83 biomarkers of neural activity in PFC (Dayas et al., 2007, Groblewski et al., 2012, Pfarr et
84 al., 2015). More recent reports suggest a critical role for the PFC in alcohol extinction
85 learning (Keistler et al., 2017, Cannady et al., 2017), suggesting that this brain region
86 may be critically involved in ‘remapping’ associations between alcohol-associated

stimuli and the motivational properties of alcohol. Thus, preclinical rodent and human data converge to implicate altered function of PFC in AUD.

The PFC has also long been known to be involved in the regulation of executive processes required to guide reward-based decision-making (Bechara, 2005, Ridderinkhof et al., 2004, Krawczyk, 2002), and animal studies are beginning to shed light on the computational processes that underlie these decisions (Dalley et al., 2004, Fitoussi et al., 2015). Decisions to initiate (or suppress) reward-directed motor actions are encoded in frontal-parietal circuits (Andersen and Cui, 2009), and, in the PFC, the encoding of these actions are evident prior to action initiation indicating behavioral intent (Sakagami and Niki, 1994, Sakagami and Tsutsui, 1999, Tanji and Hoshi, 2001, Momennejad and Haynes, 2013, Boulay et al., 2016, Andersen and Cui, 2009). These data motivated our hypothesis that similar neurocomputational processes exist in the PFC that regulate alcohol intake decisions. The implications of identifying and understanding processes that underlie the intention to use alcohol cannot be overstated, because intention signals that arise prior to alcohol seeking/drinking may be particularly effective targets for interventions aimed at reducing or eliminating alcohol consumption.

The data presented herein are novel in-depth analyses of previously published data (Linsenbardt and Lapish, 2015). In this previous study, we assessed neural firing at longer time-scales (e.g. > 1 min), which is better suited to detect pharmacologically driven effects. The goal of the current study was to examine neural activity at shorter time scales (e.g. < 1 min), to assess decision-making dynamics. To first determine if the signals reflecting the intention to drink alcohol were present in the PFC, the current

study evaluated neural activity across populations of neurons recorded during alcohol drinking in well-trained, high drinking, rats. We were particularly interested in the impact of alcohol-associated cues on drinking intent, and the role of family history of alcohol drinking on these cue-elicited decisions, as these factors have been shown to be critically important in human clinical studies (see above) and were previously unexplored. Thus, we used Indiana alcohol-preferring 'P' rats, which are a well-validated preclinical model of familial risk for excessive drinking (i.e. 'family-history positive'), and a comparison strain with no family history, Wistar rats. We hypothesized that the intention to drink or abstain would be encoded in populations of neurons in the PFC. Furthermore, since individuals with a positive family history display greater PFC responses to alcohol associated stimuli (Kareken et al., 2010, Tapert et al., 2003), we also hypothesized that P rats would display a more robust intention signal compared to Wistar.

Materials and Methods

Animals

P rats have been selectively bred for > 75 generations for their high drinking phenotype (Bell et al., 2006, Li and McBride, 1995, McBride et al., 2014), and are conceptually analogous to individuals with generations of family history of excessive drinking (i.e. family history positive). As P rats were originally derived from Wistar rats, we opted to use this population (which is 'family history negative') to assess possible family history effects.

Male P rats (N=22) were ordered from the Indiana Alcohol Research Center Animal Production Core (Indianapolis, IN), and male Wistar rats (N=21) were ordered from Envigo (Indianapolis, IN). All animals were shipped via truck to our vivarium, and were single housed and placed on a 12 hour reverse light/dark cycle. Animals were ≈70 days of age prior to testing and had *ad lib* access to food and water. All procedures were approved by the Animal Care and Use Committee and conformed to the Guidelines for the Care and Use of Mammals in Neuroscience and Behavioral Research (National Academic Press, 2003).

Intermittent Alcohol Procedure (IAP)

The procedural timeline and methods for these experiments have been recently described in detail (Linsenbardt and Lapish, 2015). All animals first underwent an IAP using previously published procedures (Simms et al., 2008): Rats were given access to 2 bottles, one containing 20% alcohol (v/v) and the other tap water, for 24 hours every other day (Mon/Wed/Fri) in the home cage. These procedures were continued for 4 weeks; animals had 12 total 24-hour alcohol/water access sessions.

2-Way Cued Access Protocol (2CAP)

Twenty-four hours following the final (12^{th}) IAP access session animals received access to an unsweetened 10% alcohol (v/v) solution for 2CAP sessions. 2CAP sessions occurred during the dark phase of the light/dark cycle, starting 1-3 hours after lights off. The conditioning box configuration is illustrated in Figure 1A. During 2CAP, a white stimulus light was illuminated for 2 seconds on one side of the rectangular box at

155 random. One second after this light was turned off, a sipper tube containing 10%
156 alcohol (v/v) solution was extended into the box on the same side as the light cue. Thus,
157 the light was a Discriminative Stimulus (DS+) that predicted the location that the alcohol
158 was to be made available. To ensure the sipper motor sound did not serve as a
159 directional cue, both tube motors were turned on for the same duration, but only the
160 appropriate sipper entered the chamber. The tube was available for ≈10 seconds. Each
161 trial was separated by a 20-180 second inter-trial interval (ITI; 90 seconds on average;
162 randomized order). A total of 40 trials were conducted for 5 out of 7 days a week
163 (weekdays) for 3 weeks (15 total sessions) prior to surgery. Water sessions were
164 identical to alcohol sessions except the sippers contained water. During water sessions,
165 a tube containing 10% (v/v) alcohol was present outside the fluid delivery port to ensure
166 that the presence or absence of the alcohol odor did not predict alcohol
167 availability/unavailability.
168
169 Stereotaxic Surgery and Behavioral Electrophysiology
170 Following the 15-day acquisition/maintenance of 2CAP, a group of Wistar (N=3)
171 and P rats (N=4) with matched 15-day 2CAP alcohol consumption history (P = 1.31 ±
172 0.06; Wistar = 1.25 ± 0.06; mean g/kg ± SEM) were selected for electrophysiological
173 experiments, and were unilaterally implanted with multi-tetrode arrays in the mPFC
174 (Linsenbardt and Lapish, 2015). This matching was conducted for 3 principle reasons.
175 First, the use of rats that will reliably consume/self-administer excessive amounts of
176 alcohol under limited access conditions is a prerequisite to identifying how such alcohol
177 consumption alters neurophysiological processes - it is not possible to assess the

effects of alcohol consumption in populations that do not drink alcohol. Second, matching for alcohol consumption reduced the possibility that any observed differences in physiology were not simply due to differences in alcohol experience. Finally, these matched populations of rodents are directly comparable to human studies in which groups of family history positive and family history negative individuals are matched for drinking history (Kareken et al., 2010).

After a full recovery from surgery, animals were given a period of one week of habituation/acclimation prior to electrophysiological recordings. Animals were habituated to the handling required for incremental lowering of tetrodes prior to the task, and also to navigating the 2CAP environment with the tether connecting the implanted electrode array to the recording hardware. After this habituation period, ≈3 days of 2CAP reinforced with 10% alcohol (v/v) were conducted while electrophysiology was recorded using a 96 channel electrophysiological recording system (Neuralynx, Bozeman, MT). Animals were then given ≈3 water sessions where the sippers contained water. A primary goal of these water sessions was to make a direct connection to studies of brain function in humans, wherein alcohol-associated cues are presented in the absence of access to alcohol (Kareken et al., 2010). Electrodes were lowered 50-100μm prior to each recording session to collect data from new neuronal ensembles. Following the completion of behavioral testing and electrophysiological recordings, placements were verified via histology (reported in Linsenbardt and Lapish, 2015).

Spike trains were manually identified and sorted into individual cell clusters based on the features of the waveform in Spike Sort 3D (Neuralynx, Bozeman, MT).

After cell sorting, duplicate timestamps and inter-spike intervals <3 msec were removed from spike trains. Only spike trains containing >150 spikes were analyzed.

Video Tracking/Behavioral Monitoring:

One video camera was used in conjunction with ANY-maze software (Wood Dale, IL) to track the head location of animals while they performed the task, and another was used to record high-definition video and audio to identify trials where animals ultimately consumed fluid (drinking trials; Figure 1B) or did not (non-drinking trials; Figure 1C). Drinking trials were assessed offline and defined as trials where at least one 'lick' occurred. A lick was detected by the combination of the animals behavior and the sound of the ball-bearing sippers that were clearly audible in the video recordings. Digital XY coordinates were converted to voltage and fed directly into electrophysiology hardware where they were recorded in parallel to neuronal activity. Raw tracking values were used to plot the location of the animals within the conditioning apparatus.

Experimental Design and Statistical Analysis:

Behavioral statistics: Detailed behavioral results for animals used in electrophysiology studies were recently described (Linsenbardt and Lapish, 2015). Behavioral analyses for the current work were primarily focused on time-locked changes in locomotor behavior in response to the various task stimuli. We were particularly interested in determining if there were differences in behavior between trials in which animals ultimately drank fluid, or did not, as these differences may be related to (or

224 mediated by) computations in the PFC encoding drinking decisions. Head movement
225 speed was positively skewed, so it was first log transformed to normalize. We next
226 evaluated differences between movement speed on a bin-by-bin basis using rank-sum
227 tests, which were followed by Benjamini Hochberg FDR correction for multiple
228 comparisons. The number of drinking and non-drinking trials were analyzed using two-
229 way repeated measures ANOVA with rat population (P vs . Wistar) as the between
230 groups factor and number of drinking/non-drinking trials as the within-subjects factor.

231 *General electrophysiology statistics*: The results of firing rate over the course of
232 the entire 2CAP sessions for electrophysiology studies were recently described
233 (Linsenbardt and Lapish, 2015). The primary goal herein was to evaluate *cue-induced*
234 alterations in neural activity, which was not evaluated previously. Peri-stimulus time
235 histograms (PSTHs) were created by aligning binned (100ms) spike trains for each
236 neuron to the onset of each trial. PSTHs were smoothed using a Gaussian function with
237 a standard deviation of 300 milliseconds, and softmax normalized to avoid being biased
238 by high firing rate neurons by dividing the firing rate of each neuron by its maximum
239 variance (Ames et al., 2014).

240 *Stimuli/Task Responsiveness of Individual Neurons*: A signal-to-noise statistic
241 (d-prime, d´) was used to quantify the degree to which each neurons activity changed in
242 response to the task stimuli compared to pre-task (baseline) activity as well as chance
243 (surrogate testing); binned (100ms) spike trains were not transformed or normalized in
244 any way prior to these analyses. Individual neurons were evaluated for the degree of
245 responsiveness using d´ (Gale and Perkel, 2010, Barr et al., 2010). Specifically, d´ was
246 calculated by dividing the absolute values of the mean difference between firing rate

247 during the baseline epoch and the rest of trial by the square root of the sum of their
248 squared deviations. To evaluate the significance of the d´ values, surrogate data were
249 created by taking each neurons spike train and randomly shuffling it 500 times. d´ was
250 then determined for each of the 500 randomly shuffled spike trains and these values
251 were used to compute a 95% confidence interval of the null distribution for each neuron.
252 To evaluate differences in d´ on drinking vs. non-drinking trials, a two-way ANOVA was
253 conducted with responsiveness group (drinking sig., non-drinking sig., both sig.) and
254 trial type (drinking and non-drinking trials) as factors, which was followed by Sidak-
255 corrected post-hoc comparisons. To evaluate proportions of responsive neurons in P vs
256 Wistar rats, Chi-squared (χ^2) analyses were conducted on alcohol and water sessions
257 separately.

258 *Mutual Information of individual neurons*: Following d´ analyses, we next used
259 mutual information (an information theoretic statistical approach (Cover and Thomas,
260 2005, Timme and Lapish, 2018) to precisely quantify the total *amount* of information
261 encoded by each neuron. This approach is preferable to other parametric statistical
262 analysis of firing rate, as firing rate distributions are highly non-normal (Roxin et al.,
263 2011, Timme et al., 2016). We focused these analyses on two categorical domains –
264 the amount of information encoding real trials vs null trials (collectively referred to as
265 trial-encoding), and the amount of information encoding drinking trials vs non-drinking
266 trials (collectively referred to as drink-encoding). Null trials were constructed from
267 periods of the neural recording that were randomly selected from the inter-trial interval
268 such that full null trials did not overlap real trials at any time.

We began the mutual information calculation by aligning the first 10 drinking, the first 10 non-drinking, and 20 null trials relative to the cue onset (drinking and non-drinking trials) or a randomly chosen time point during the inter-trial interval (null trials). Null trials were constructed from periods of the neural recording that were randomly selected from the inter-trial interval such that full null trials did not overlap real trials at any time. At a given time bin *t* relative to the stimulus onset time and for a given neuron *i*, we constructed a joint discrete probability distribution $p_{i,t}(x,y)$, where *x* was the discretized smoothed spiking rate of the neuron (see above, 100 ms bins relative to stimulus onset) and *y* was either the trial type (real vs. null) or the drink outcome (drinking trials vs. non-drinking trials). The smoothed spiking rate of the neuron was discretized such that the values across trials were ranked and binned into three states (low, medium, or high firing) with equal number of counts (or as close to equal as possible in the event of tied values). The probability was then calculated by dividing the number of joint state observations by the total number of trials. For instance, in the case of drink outcome encoding, for a given neuron and time bin, we may have observed 5 joint states in which the neuron had a low firing rate during drinking trials. In this example, $p_{i,t}(x = \text{low},y = \text{drinking}) = 5/20 = 0.25$. In the case of stimulus encoding, we might have observed 7 joint states in which the neuron had a high firing rate during real trials. In this example, $p_{i,t}(x = \text{high},y = \text{real}) = 7/40 = 0.175$. Note that drink encoding only utilized real trials, so only 20 total observations where performed, whereas trial encoding utilized both real and null trials, resulting in 40 total observations.

For each neuron, time bin, and encoding type (drink encoding and trial encoding), we calculated the mutual information using Eq. 1:

$$I_{i,t}(x,y) = \sum_{x,y} p_{i,t}(x,y) log_2 \left(\frac{p_{i,t}(x,y)}{p_{i,t}(x) p_{i,t}(y)} \right) \quad \text{(Eq. 1)}$$

We used base 2 for the logarithm in Eq. 1 to produce mutual information results in units of bits. In Eq. 1, the marginal discrete distributions $p_{i,t}(x)$ and $p_{i,t}(y)$ are found by summing over the other variable:

$$p_{i,t}(x) = \sum_y p_{i,t}(x,y),\ p_{i,t}(y) = \sum_x p_{i,t}(x,y) \quad \text{(Eq. 2)}$$

The mutual information quantifies how much information one variable provides about the other. In this case, if a neuron tends to fire much more frequently on drinking trials than non-drinking trials, for instance, a large mutual information value would result. However, if drinking status and neuron firing rate were unrelated, then a small mutual information value would result. By calculating the mutual information at each time bin for each neuron, we were able to evaluate encoding dynamically throughout the task.

Due to the discrete nature of experimental trials and the fact that mutual information results cannot be lower than 0, noise tends to bias mutual information results upwards (Panzeri et al., 2007, Treves and Panzeri, 1995). To assess the likelihood that a given mutual information result is not simply the result of noise, we calculated a p-value for each mutual information result by randomizing the joint observations 100 times and recalculating the mutual information for these null surrogates. The randomization procedure preserved the marginal distributions. The p-value was then calculated as the proportion of null surrogates with a mutual information result greater than or equal to the observed value in the real data. In the case where all null mutual information values were less than the result from the real data, the p-value was set to 0.005 = 0.5*(1/100) due to the resolution associated with using 100 null surrogates.

Next, to ensure that non-significant mutual information values did not inflate the estimates of standard error, the p-values were used to calculate a weight (w) for each mutual information result via $w = -\log_{10}(p)$. These weights were then normalized by dividing each weight by the sum of all the weights and used to calculate the weighted mean (Eq. 3) and standard error of the weighted mean (Eq. 4) across all relevant neurons (animal strain and liquid type) at a given time bin t.

$$\bar{I}_{w,t}(x,y) = \sum_i w_i I_{i,t}(x,y) \quad \text{(Eq. 3)}$$

$$SEM_{w,t}(x,y) = \sigma_t \sqrt{\sum_i {w_i}^2} \quad \text{(Eq. 4)}$$

In Eq. 4, σ_t is the standard deviation of the mutual information values across all neurons at the given time bin t. Therefore, large mutual information values that were unlikely to be due to chance received large weights and factored heavily into the weighted mean. In the case where the mutual information results had similar weights, the standard error of the weighted mean approached the standard error of the mean. In the case where the mutual information results were dominated by a few highly weighted values, the standard error of the weighted mean approached the standard deviation.

While the weighting procedure above allowed us to highlight the importance of significant information results, in time bins where few significant information results were observed, an upwards bias in the information results would still be observed. To detect cases where the *ensemble* of information values were not significantly different from null, we also used a KS-test to compare the distribution of real mutual information results to the distribution of mutual information results from null surrogate data used to calculate the individual neuron p-values. This allowed us to assess the time bins for which the entire ensemble of neurons was not significantly different from null data,

suggesting the ensemble as a whole was not encoding significant amounts of information (e.g., open circles Figures 3 and 4). We applied a threshold of $p < 0.01$ to all such KS-tests to assess significant ensemble encoding.

Finally, to compare information results between animal populations (P vs Wistar), we used a bootstrap approach to compare the weighted mean mutual information between P and Wistar rats at each time bin. We compared the difference between the weighted mean mutual information values in the real data to the difference weighted mean mutual information results from 10000 randomized trials (identity of P and Wistar neurons randomized preserving number of neurons in each group). The p-value was then calculated as the proportion of randomized trials with differences greater than or equal to the difference in the real data, accounting for the sign of the difference. In the case where all randomized trial difference values were less than the result from the real data, the p-value was set to 0.00005 = 0.5*(1/10000) due to the resolution associated with using 10000 randomized trials. These p-values were then corrected for multiple comparisons across time bins within a given figure using False Discover Rate control (Benjamini and Hochberg, 1995).

Principle component analysis (PCA): PCA was conducted to evaluate the predominant population-level firing rate dynamics. PCA is commonly used as a dimensionality reduction tool that requires minimal assumptions of the data (Cunningham and Yu, 2014). A single 'omnibus' PCA was conducted on a matrix containing all data for all groups so that every possible comparison could be made statistically. This matrix included ensemble activity on drinking trials, non-drinking trials, and equally sized, randomly sampled data vectors (previously described null trials).

Neural population State-Space (SS) analyses: For state-space analyses, neural population activity was projected onto the first 3 PCs of PCA space. These analyses allowed us to determine the time course of alterations in the pattern of firing rate. Similar patterns of population activity reside close to each other in 3-dimensional space, and when different are further apart. Differences in distance between 3-dimensional population activity vectors were evaluated on a bin-by-bin basis via Euclidean distance analyses (Ames et al., 2014). The mean distance between each trial and every other trial in that comparison type were made (for example drinking trial 1 vs all null trials, drinking trial 2 vs all null trials, etc.), and the mean and variance of the (non-redundant) distances were used for plotting and statistical analyses. We were specifically interested in differences between drinking and non-drinking trials (vs null trials), and therefore evaluated Euclidean distance between these groups and null trials on a bin by bin bases using Benjamini Hochberg FDR-corrected rank-sum testing.

Results

Movement dissociates drinking versus non-drinking trials during fluid availability but not during stimulus (DS) presentation

To assess the neural dynamics of alcohol-associated cues within mPFC, extracellular electrophysiological activity was obtained from ensembles of neurons during performance of an alcohol-drinking task in Wistar and P rats matched for alcohol history (Linsenbardt and Lapish, 2015, McCane et al., 2014). Neural recordings were performed in well-trained animals that had > 7 weeks of prior alcohol experience. Subsequent recordings were made using identical procedures, except the alcohol

384 solution was replaced with water. The layout of the conditioning apparatus (Figure 1A),
385 as well as representative video tracking data on drinking (Figure 1B) and non-drinking
386 (Figure 1C) trials are presented in Figure 1. Head movement speed differentiated
387 drinking from non-drinking trials in both rat populations on both alcohol and water
388 sessions, primarily (or exclusively) during the fluid access epoch (Figure 1D; FDR-
389 corrected rank sum tests; p's<.05). Differences during fluid access were expected, as
390 drinking required that animals remain in close proximity to the sipper on drinking trials.
391 No differences in movement speed were observed during the DS of drinking versus
392 non-drinking trials, while transient differences were observed from the 2 to 4.5 second
393 period following DS offset (Figure 1D). Furthermore, no differences (main effects or
394 interactions; p's > 0.20) were observed in the mean number of drinking (# trials ± SEM:
395 P = 19.19 ± 1.31; Wistar = 22.40 ± 2.03) or non-drinking trials (# trials ± SEM: P =
396 20.50 ± 1.34; Wistar = 17.60 ± 2.03). Collectively these data indicate that the behavioral
397 response to the DS was not predictive of a drinking trial.
398
399 *Task stimuli elicited differential responsiveness in neurons on drinking trials versus non-*
400 *drinking trials.*
401 To determine if firing rates of individual neurons differed on drinking vs. non-
402 drinking trials, the changes in firing evoked by the presentation of trial-associated stimuli
403 (e.g., DS, sipper) was compared to a baseline period 2 seconds immediately before the
404 trial (Figure 2A). Heterogeneity in the firing rates evoked by task stimuli varied greatly
405 between neurons, with some showing both increases and decreases in firing rate
406 (Figure 2B1), and others displaying only decreases (Figure 2B2) or increases (Figure

2B3). The signal-to-noise statistic d´ was used to identify stimulus responsive neurons, and out of 520 neurons across both groups of rats, 179 (≈34%) displayed statistically significant changes in d´ (Figure 2A+C). Neurons were observed that responded to task-associated stimuli similarly on drinking and non-drinking trials (Figure 2D, purple group). Additionally, subgroups of neurons were then identified that were influenced by task stimuli *only* on drinking trials or non-drinking trials (Figure 2D red and blue groups, respectively). Comparisons of drink-encoding neurons confirmed that non-drinking trial responsive neurons displayed lower responsiveness on drinking trials. The converse was also true; the subgroup of drinking trial responsive neurons displayed lower responsiveness on non-drinking trials (two-way ANOVA; $F(2,679)=38.03, p<0.0001$; Figure 2D inset). Interestingly, a greater number of responsive neurons were found when drinking status was taken into account compared to when it was ignored (225 vs 179; Figure 2F), with no significant differences in the proportions of neuron response between P and Wistar rats on either alcohol ($\chi^2=3.24$; $p=0.20$) or water sessions ($\chi^2=2.34$; $p=0.31$; Figure 2E). Thus, mPFC neurons were found that possessed the capacity to encode decisions and/or behaviors associated with drinking/non-drinking trials.

P rats exhibit diminished drink-encoding

To quantify and compare the *amount* of information encoded by trial- and drink-encoding neurons over time, information theoretic statistical approaches were used. The goal of these analyses were to capture the amount of information encoded in each neuron about the trial-associated stimuli (trial-encoding) and if the neural firing rates

dissociated drinking/non-drinking trials (drink-encoding). Additionally, these analyses focused on drink-encoding that occurred *prior* to fluid availability (the 0 - 4.5 second interval), as this time interval was expected to contain cue-elicited encoding of the intention to drink or abstain. In addition to quantifying the amount of information using mutual information (MI), these analyses captured different encoding strategies (e.g., firing rate increases or decreases) at each time bin during a trial (e.g., encoding during the DS vs. encoding during access).

Examples of trial-encoding neurons are plotted in Figure 3A1-3. There was marked heterogeneity in trial-encoding. The neurons in Figure 3A1+A3 encoded trial stimuli with increases in firing rate, whereas the neuron in Figure 3A2 did so with decreases in firing rate. The neurons in Figure 3A1+A3 displayed differences from one another in the encoding of the sipper retracting. Additionally, the neurons in Figure 3A2+A3 encoded both visual (light) and auditory stimuli (sipper entry), compared to the neurons in Figure 3A1 which primarily encoded visual (DS) stimuli. Collectively, the neurons recorded from Wistar's exhibited stronger trial-encoding than P's during alcohol sessions (FDR-corrected rank sum tests; p's<.05; Figure 3B), whereas no differences were observed in trial-encoding during water sessions (FDR-corrected rank sum tests; p's<.05; Figure 3C).

Examples of drink-encoding neurons are plotted in Figure 4A1-3. As with trial-encoding, neurons displayed heterogeneity in the magnitude and location of drink-encoding. The neurons in Figure 4A1+A3 encoded drinking intent (pre-fluid availability drink-encoding), whereas the neuron in Figure 4A2 encoded drinking only following fluid availability. The neurons in Figure 4A1-A3 displayed differences from one another in the

453 encoding of drinking during/following fluid removal. Collectively, neurons recorded from
454 Wistar rats encoded more information than P's about drinking/non-drinking trials prior to
455 alcohol access vs P rats (FDR-corrected rank sum tests; p's<.05; Figure 4B), which may
456 indicate that the mPFC of Wistar rats performed computations associated with
457 subsequent drinking; such as the intention to drink. In contrast, there were little to no
458 differences in drink-encoding across rat populations prior to water availability (FDR-
459 corrected rank sum tests; p's<.05; Figure 4C).
460
461 *Neural activity patterns in populations of mPFC neurons reflect the intention to drink in*
462 *Wistar, but not P, rats*
463 In order to determine if differences in information encoding observed at the single
464 neuron level were maintained at the population level, state-space analyses were
465 performed to quantify how neural activity patterns, captured via principle components,
466 evolved throughout a trial. To quantify the evolution of neural trajectories, Euclidean
467 distance to a corresponding time bin of a null trial was computed for drinking, non-
468 drinking, and null trials (note: a given null trial was compared to all other null trials to
469 compute distance). Euclidean Distance was calculated from a multidimensional space
470 that was defined by the first 3 principle components. Larger values of Euclidean
471 distance correspond to larger differences in neural activity patterns, which indicate that
472 the predominant patterns of neural firing were different for two comparisons (Figure 5A).
473 Videos1-4 for each comparison group are provided to illustrate the evolution of neural
474 trajectories over time for each trial. During alcohol sessions, alcohol-associated cues
475 elicited neural activity patterns that diverged prior to the availability of alcohol when

476 drinking- versus non-drinking trials were compared in Wistar (FDR-corrected rank sum
477 tests; p's<.05; Figure 5B), but not P rats (FDR-corrected rank sum tests; p's<.05; Figure
478 5C). In other words, the temporal evolution of neural activity patterns in Wistar rats in
479 response to alcohol-associated cues were predictive of future drinking/non-drinking
480 trials, whereas the neural activity patterns in P rats were not. Additionally, during water
481 sessions, population activity only briefly differentiated drinking trials from non-drinking
482 trials in Wistar (FDR-corrected rank sum tests; p's<.05; Figure 5D), and failed entirely in
483 P rats (FDR-corrected rank sum tests; p's<.05; Figure 5E). In contrast, there were large
484 differences between P and Wistar in cue/task-elicited population activity. Specifically, on
485 water drinking trials, P rats displayed greater alterations in neural activity patterns vs
486 Wistar rats (FDR-corrected rank sum tests; p's<.05; Figure 6A). Thus, in P rats, the
487 mPFC was biased toward encoding alcohol drinking during alcohol consumption,
488 whereas in Wistar rats, encoding of the intention to drink alcohol *and* alcohol drinking
489 was present. Therefore, converging evidence suggests that the encoding of alcohol
490 drinking intent is impaired in the mPFC of P rats, which may contribute to the
491 predisposition for excessive alcohol consumption.
492
493 **Discussion**
494 The goal of the current study was to determine if the intent to drink alcohol was
495 encoded by populations of neurons in the rodent mPFC, and if such encoding was
496 influenced by a family history of alcohol drinking. Task-stimuli-evoked changes in neural
497 activity were observed in mPFC of both strains of rats (Figure 2). Contrary to our
498 hypothesis, during alcohol sessions, patterns of neural activity at both the single neuron

and population levels more robustly disambiguated drinking from non-drinking trials in Wistar rats. Importantly, these differences were observed *prior to the availability of alcohol,* possibly reflecting the intent to drink (Figures 4B+ 5B). Additionally, during alcohol sessions, enhanced trial-encoding was observed in Wistar rats (Figure 3B), whereas during water sessions, task-stimuli-evoked changes in neural population activity was larger in P rats (Figure6A). Collectively, these data suggest that differences in family history of excessive drinking may alter the computations performed by mPFC that control alcohol drinking, either directly, or as a consequence of an interaction between inherited/genetic differences and moderate (but similar) alcohol history.

In water sessions, P rats more robustly encode alcohol-associated stimuli

P rats are an extremely well-validated rodent model of AUD (McBride and Li, 1998, McBride et al., 2014, Bell et al., 2014, Lumeng and Li, 1986, Gatto et al., 1987, Stewart et al., 1991, Kampov-Polevoy et al., 2000, Waller et al., 1982). One feature that sets these animals apart from other rodent populations that willingly consume alcohol, is their robust seeking phenotype (Czachowski and Samson, 2002). Given this, it was surprising to find that during alcohol seeking/consumption, trial-encoding was weaker in P's (Figure 3B). Weaker trial-encoding in P's did not result in an opportunity cost, as there were no differences in the number of drinking trials or volume of fluid consumed between Wistar and P rats. However, differences in drinking were intentionally minimized across Wistars and P's, as each animal was selected to control for differences in behavior and, especially, history of alcohol intake (Linsenbardt and Lapish, 2015). Since differences in trial-encoding were not associated with increased

seeking or drinking when reinforced with alcohol, it does not likely reflect the motivational salience of the stimuli or more basic features of the stimuli such as its perceived intensity or information required to locate/time the delivery of the reinforcer.

Several studies have found that P rats display persistent alcohol-seeking behavior in the presence of cues previously associated with alcohol access/consumption compared to other strains (Czachowski and Samson, 2002, Ciccocioppo et al., 2001, Linsenbardt and Lapish, 2015). This suggests that alcohol-associated stimuli retain their motivational properties in P rats when alcohol is not available. Consistent with this hypothesis, the only comparison where P's exhibited stronger encoding than Wistars to cues preceding fluid availability was during water sessions at the neural population level (Figure 6A). This observation may reflect the conflict-driven recruitment of mPFC in response to the violation of the previously acquired association between trial-associated stimuli and alcohol experience. Alternatively, enhanced stimuli-encoding during water sessions may reflect the 'cached' value of alcohol-associated cues based on prior experiences with alcohol/stimuli rather than their current value (Dezfouli and Balleine, 2013, Daw et al., 2005, Doya, 1999, Rangel et al., 2008, Redish et al., 2008). Consistent with this, an enhanced BOLD response to alcohol associated stimuli in those with increased familial risk for an AUD versus those not at risk has only been observed in a similar setting in which alcohol-associated stimuli are presented in the absence of alcohol access/exposure (Kareken et al., 2010).

Encoding of the intent to drink alcohol in mPFC is diminished in P rats

In the current study, the encoding of drinking intent (e.g., drink outcome specific changes in neural activity *prior* to drinking) was diminished in mPFC of P rats compared to Wistar rats. While, these data are the first to provide evidence that mPFC neurons directly encode the intent to consume alcohol, they also indicate this signal is diminished in animals with increased risk of excessive drinking. These data suggest that increased familial risk diminishes the contribution of the mPFC in the decision to seek and drink alcohol. However, there is also substantial evidence for transitions in encoding in subcortical brain regions, such as the striatum. The dorsomedial striatum directly influences alcohol consumption that is still sensitive to devaluation (i.e., not 'habitual'), whereas the dorsolateral striatum modulates alcohol consumption only after prolonged training in which animals have become insensitive to devaluation and display habitual behavioral responding (Corbit et al., 2012). Thus, over the course of repeated alcohol drinking experiences, there is a reorganization of the neural circuits that regulate alcohol drinking behavior. Taken together, these studies underscore the need to disambiguate the distinct roles played by alcohol and family history on the neural circuits that regulate devaluation insensitive and/or aversion-resistant drinking; issues not directly addressed in the current studies.

Summary/Conclusions

Collectively, the data provided herein indicate differences in the role of the mPFC in alcohol consumption between populations with or without increased familial risk of excessive drinking. This finding is characterized by two primary features observed in P rats: 1) The encoding of the decision to drink is blunted during alcohol drinking, and 2)

The encoding of stimuli previously associated with alcohol is enhanced during water sessions. We have also observed that neurons in the mPFC of P rats may be uniquely sensitive to the alcohol-associated context of the 2CAP conditioning chamber (i.e. prior to task; (Linsenbardt and Lapish, 2015). The expression of these features was observed in animals that exhibit an inherited risk for excessive drinking, which may reflect underlying differences in neurobiology that facilitate persistent alcohol seeking and/or the transition to aversion-resistant drinking. Identifying strategies to restore the contribution of the mPFC in the intention to drink alcohol and blunt the encoding of alcohol associated cues observed in water sessions may provide effective targets to treat an AUD. Importantly these data further highlight the need to consider inherited/genetic risk factors when developing treatment strategies for AUD's.

Figure Legends

Figure1. Movement dissociates drinking versus non-drinking trials during fluid availability but not during stimulus (Discriminative Stimulus; i.e. cue light) presentation. **(A)** Configuration of conditioning boxes used for cue-induced drinking/neurophysiology. Representative traces of head location within the conditioning box on drinking trials **(B)** and non-drinking trials **(C)** from a single session in a Wistar rat given alcohol solution. Illustrations at the top of all figure panels in **(D1-4)** illustrate the timecourse of stimuli presentation on each trial. Two seconds of 'baseline' data precede the start of each trial, in which a light was illuminated for 2 seconds on one side of the two-sided chamber. A one second 'delay' in which no stimuli were activated bridged the light cue and the

initiation of sipper movement into the chamber. Sipper movement is represented by the two gray arrows, with the first arrow indicating sipper entry, and the second arrow indicating sipper removal. Fluid was readily available (only on the chamber side cued by the light) between the end of the sipper motor entry (first arrow) and the start of the sipper motor removal (second arrow). **(D1-4)** Mean (±SEM) log-transformed head movement speed changed significantly over time on drinking trials compared to non-drinking trials in P and Wistar rats on both alcohol and water sessions. Green bars denote drinking vs non-drinking trial differences (FDR-corrected rank sum tests; p's<.05).

Figure2. Task stimuli elicited varied responses in neurons on drinking trials versus non-drinking trials, illustrating the capacity to encode/predict future drinking. (**A**) The z-scored timecourse of alterations in firing rate in each of the 179 neurons with significant firing rate alterations (ignoring drinking vs non-drinking status) sorted from lowest baseline firing rate (top) to highest baseline firing rate (bottom). (**B1- B3**) Peri-stimulus time histograms (PSTHs) of 3 representative neurons recorded from a Wistar rat during the same alcohol access session; all displayed significant alterations in firing rate (see panel C). (**C**) Approximately 1/3 of all neurons displayed significant alterations in firing rate vs. baseline as measured by d´ (ignoring drinking vs non-drinking status). (**D**) Significant individual neuron d´ scores on only drinking trials (red), only non-drinking trials (blue), and both drinking and non-drinking trials (purple). Square symbols represent data from Wistar rats and Circle symbols represent data from P rats. The mean of d´ scores on drinking vs non-drinking trials from these subgroups was as expected (inset); drinking-responsive neurons had lower d´ values on non-drinking trials, and non-drinking-responsive neurons had lower d´ values on drinking trials. (Two-way ANOVA; $F(2,679)=38.03, p<0.0001$;). *'s in inset indicate significantly lower d´ scores from other two comparison groups (Sidak's multiple comparisons adjusted p's<.01). (**E**) The proportion of neurons displaying significant d´ values (drinking/non-drinking/both) were similar between P and Wistar rats (Chi-squared p's≥0.20). (**F**) When data were evaluated independently of drinking status (top) a smaller proportion of neurons demonstrated selectivity to presentation of environmental stimuli (≈33%) than when selectivity was assessed taking drinking/non-drinking trials into account (bottom, ≈43%).

Figure3. P rats exhibit blunted trial encoding during alcohol sessions. (**A1- A3**) Mean firing rate of 3 representative trial encoding neurons. Neurons in **A1+A3** (Wistar/Alcohol and P/Water) encoded trial stimuli with increases in firing rate, whereas neuron in **A2** (Wistar/Alcohol) did so with decreases in firing rate. Neurons displayed significant heterogeneity in the magnitude and location of trial encoding. For example, neurons in **A1+A3** displayed differences in the encoding of the sipper retracting. Also, **A2+A3** encode both visual and auditory stimuli. On average, Wistar neurons encoded more

information about trial stimuli than P during alcohol sessions **(B)**, whereas no differences were observed between P and Wistar during water sessions **(C)**. Data represent weighted mean ± standard error of the weighted mean. Green *'s represent FDR corrected differences between P and Wistar ($p < 0.01$). Open circles represent time bins where the ensemble of neurons did not produce significant encoding.

Figure4. P rats exhibit diminished drink encoding during alcohol sessions. (**A1- A3**) Mean firing rate of 3 representative drink encoding neurons. Neurons in **A1+A3** (Wistar/Water and Wistar/Alcohol) encoded drinking intent (pre-fluid availability drink encoding), whereas neuron in **A2** (P/Alcohol) encodes drinking only during fluid availability. As with trial encoding, neurons displayed significant heterogeneity in the magnitude and location of drink encoding. For example, neurons in **A1-A3** displayed differences in the encoding of drinking during/following fluid removal. On average, Wistar neurons encoded more information about drinking/non-drinking than P during alcohol sessions **(B)**, whereas inconsistent/transient differences were observed between P and Wistar during water sessions **(C)**. Data represent weighted mean ± standard error of the weighted mean. Green *'s represent FDR corrected differences between P and Wistar ($p < 0.01$). Open circles represent time bins where the ensemble of neurons did not produce significant encoding.

Figure5. mPFC neural activity patterns reflect the intention to drink alcohol in Wistar, but not P, rats. **(A)** Illustrates neural trajectories in 3-dimensional Euclidean space on a single drinking (red), non-drinking (blue), and null trial (black). Filled green circles indicate the same time bin across each of the conditions, with the Euclidean distance between drinking (0.67) and non-drinking (0.59) trials from null used for statistical analyses in **B-E**. **(B)** Populations of neurons in Wistar rats on alcohol access sessions encoded the intent to drink or not drink – differences in the pattern of firing between drinking/non-drinking trials were observed prior to alcohol access. **(C)** Populations of neurons in P rats on alcohol access sessions encoded drinking/non-drinking, but did not encode alcohol drinking intent. **(D)** Populations of neurons in Wistar only transiently encoded water drinking. **(E)** Populations of neurons in P failed to encode water drinking or water drinking intent. Data are presented as mean ±SEM. Green |'s represent FDR corrected differences in Euclidean Distance between drinking and non-drinking trials ($p < 0.05$).

Figure6. mPFC neural activity patterns more robustly encode alcohol-associated stimuli than Wistar during water sessions. Data presented in this figure are identical to those found in figure 5D+E, and are presented here to illustrate P vs. Wistar differences. **(A)** On drinking trials during water sessions, population of neurons in P rats better encoded alcohol-associated task/stimuli than Wistar rats, whereas there were no differences in encoding of task/stimuli between P and Wistar on non-drinking (water) trials **(B).** Data

are presented as mean ±SEM. Green |'s represent FDR corrected differences between P and Wistar ($p < 0.05$).

Videos:S1-4. The top panel in all videos is identical to data found in Figure 6. The bottom panel was generated using DataHigh software (Cowley et al., 2013), and represents the timecourse of neural trajectories over the course of drinking trials (red), non-drinking trials (blue), and null trials (black), in three-dimensional (Euclidean) space. **Video_S1** represents data from Wistar rats given alcohol access; **Video_S2** represents data from P rats given alcohol access; **Video_S3** represents data from Wistar rats given access to Water; **Video_S4** represents data from P rats given access to Water.

References

AMES, K. C., RYU, S. I. & SHENOY, K. V. 2014. Neural dynamics of reaching following incorrect or absent motor preparation. *Neuron,* 81**,** 438-51.

ANDERSEN, R. A. & CUI, H. 2009. Intention, action planning, and decision making in parietal-frontal circuits. *Neuron,* 63**,** 568-83.

BARR, R. C., NOLTE, L. W. & POLLARD, A. E. 2010. Bayesian quantitative electrophysiology and its multiple applications in bioengineering. *IEEE Rev Biomed Eng,* 3**,** 155-68.

BECHARA, A. 2005. Decision making, impulse control and loss of willpower to resist drugs: a neurocognitive perspective. *Nat Neurosci,* 8**,** 1458-63.

BELL, R. L., RODD, Z. A., ENGLEMAN, E. A., TOALSTON, J. E. & MCBRIDE, W. J. 2014. Scheduled access alcohol drinking by alcohol-preferring (P) and high-alcohol-drinking (HAD) rats: modeling adolescent and adult binge-like drinking. *Alcohol,* 48**,** 225-34.

BELL, R. L., RODD, Z. A., LUMENG, L., MURPHY, J. M. & MCBRIDE, W. J. 2006. The alcohol-preferring P rat and animal models of excessive alcohol drinking. *Addict Biol,* 11**,** 270-88.

BENJAMINI, Y. & HOCHBERG, Y. 1995. *Controlling the false discovery rate: a practical and powerful approach to multiple testing*.

BOULAY, C. B., PIEPER, F., LEAVITT, M., MARTINEZ-TRUJILLO, J. & SACHS, A. J. 2016. Single-trial decoding of intended eye movement goals from lateral prefrontal cortex neural ensembles. *J Neurophysiol,* 115**,** 486-99.

BRASS, M., LYNN, M. T., DEMANET, J. & RIGONI, D. 2013. Imaging volition: what the brain can tell us about the will. *Exp Brain Res,* 229**,** 301-12.

BUSCHMAN, T. J. & MILLER, E. K. 2014. Goal-direction and top-down control. *Philos Trans R Soc Lond B Biol Sci,* 369.

CANNADY, R., MCGONIGAL, J. T., NEWSOM, R. J., WOODWARD, J. J., MULHOLLAND, P. J. & GASS, J. T. 2017. Prefrontal cortex KCa2 channels regulate mGlu5-dependent plasticity and extinction of alcohol-seeking behavior. *J Neurosci*.

CATAFAU, A. M., ETCHEBERRIGARAY, A., PEREZ DE LOS COBOS, J., ESTORCH, M., GUARDIA, J., FLOTATS, A., BERNA, L., MARI, C., CASAS, M. & CARRIO, I. 1999. Regional cerebral blood flow changes in chronic alcoholic patients induced by naltrexone challenge during detoxification. *J Nucl Med,* 40**,** 19-24.

CICCOCIOPPO, R., ANGELETTI, S. & WEISS, F. 2001. Long-lasting resistance to extinction of response reinstatement induced by ethanol-related stimuli: role of genetic ethanol preference. *Alcohol Clin Exp Res,* 25**,** 1414-9.

CORBIT, L. H., NIE, H. & JANAK, P. H. 2012. Habitual alcohol seeking: time course and the contribution of subregions of the dorsal striatum. *Biol Psychiatry,* 72**,** 389-95.

COVER, T. M. & THOMAS, J. A. 2005. Entropy, Relative Entropy, and Mutual Information. *Elements of Information Theory.* John Wiley & Sons, Inc.

COWLEY, B. R., KAUFMAN, M. T., BUTLER, Z. S., CHURCHLAND, M. M., RYU, S. I., SHENOY, K. V. & YU, B. M. 2013. DataHigh: graphical user interface for visualizing and interacting with high-dimensional neural activity. *J Neural Eng,* 10**,** 066012.

CUNNINGHAM, J. P. & YU, B. M. 2014. Dimensionality reduction for large-scale neural recordings. *Nat Neurosci,* 17**,** 1500-9.

CZACHOWSKI, C. L. & SAMSON, H. H. 2002. Ethanol- and sucrose-reinforced appetitive and consummatory responding in HAD1, HAD2, and P rats. *Alcohol Clin Exp Res,* 26**,** 1653-61.

DALLEY, J. W., CARDINAL, R. N. & ROBBINS, T. W. 2004. Prefrontal executive and cognitive functions in rodents: neural and neurochemical substrates. *Neurosci Biobehav Rev,* 28**,** 771-84.

754 DAW, N. D., NIV, Y. & DAYAN, P. 2005. Uncertainty-based competition between
755 prefrontal and dorsolateral striatal systems for behavioral control. *Nat Neurosci,*
756 8**,** 1704-11.
757 DAYAS, C. V., LIU, X., SIMMS, J. A. & WEISS, F. 2007. Distinct patterns of neural
758 activation associated with ethanol seeking: effects of naltrexone. *Biol Psychiatry,*
759 61**,** 979-89.
760 DEZFOULI, A. & BALLEINE, B. W. 2013. Actions, action sequences and habits:
761 evidence that goal-directed and habitual action control are hierarchically
762 organized. *PLoS Comput Biol,* 9**,** e1003364.
763 DOYA, K. 1999. What are the computations of the cerebellum, the basal ganglia and
764 the cerebral cortex? *Neural Netw,* 12**,** 961-974.
765 FITOUSSI, A., LE MOINE, C., DE DEURWAERDERE, P., LAQUI, M., RIVALAN, M.,
766 CADOR, M. & DELLU-HAGEDORN, F. 2015. Prefronto-subcortical imbalance
767 characterizes poor decision-making: neurochemical and neural functional
768 evidences in rats. *Brain Struct Funct,* 220**,** 3485-96.
769 FUSTER, J. M. & BRESSLER, S. L. 2015. Past makes future: role of pFC in prediction.
770 *J Cogn Neurosci,* 27**,** 639-54.
771 GALE, S. D. & PERKEL, D. J. 2010. A basal ganglia pathway drives selective auditory
772 responses in songbird dopaminergic neurons via disinhibition. *J Neurosci,* 30**,**
773 1027-37.
774 GATTO, G. J., MURPHY, J. M., WALLER, M. B., MCBRIDE, W. J., LUMENG, L. & LI,
775 T. K. 1987. Chronic ethanol tolerance through free-choice drinking in the P line of
776 alcohol-preferring rats. *Pharmacol Biochem Behav,* 28**,** 111-5.
777 GEORGE, M. S., ANTON, R. F., BLOOMER, C., TENEBACK, C., DROBES, D. J.,
778 LORBERBAUM, J. P., NAHAS, Z. & VINCENT, D. J. 2001. Activation of
779 prefrontal cortex and anterior thalamus in alcoholic subjects on exposure to
780 alcohol-specific cues. *Arch Gen Psychiatry,* 58**,** 345-52.
781 GROBLEWSKI, P. A., RYABININ, A. E. & CUNNINGHAM, C. L. 2012. Activation and
782 role of the medial prefrontal cortex (mPFC) in extinction of ethanol-induced
783 associative learning in mice. *Neurobiol Learn Mem,* 97**,** 37-46.
784 GRUSSER, S. M., WRASE, J., KLEIN, S., HERMANN, D., SMOLKA, M. N., RUF, M.,
785 WEBER-FAHR, W., FLOR, H., MANN, K., BRAUS, D. F. & HEINZ, A. 2004. Cue-
786 induced activation of the striatum and medial prefrontal cortex is associated with
787 subsequent relapse in abstinent alcoholics. *Psychopharmacology (Berl),* 175**,**
788 296-302.
789 HAYNES, J. D., SAKAI, K., REES, G., GILBERT, S., FRITH, C. & PASSINGHAM, R. E.
790 2007. Reading hidden intentions in the human brain. *Curr Biol,* 17**,** 323-8.
791 KAMPOV-POLEVOY, A. B., MATTHEWS, D. B., GAUSE, L., MORROW, A. L. &
792 OVERSTREET, D. H. 2000. P rats develop physical dependence on alcohol via
793 voluntary drinking: changes in seizure thresholds, anxiety, and patterns of
794 alcohol drinking. *Alcohol Clin Exp Res,* 24**,** 278-84.
795 KAREKEN, D. A., BRAGULAT, V., DZEMIDZIC, M., COX, C., TALAVAGE, T.,
796 DAVIDSON, D. & O'CONNOR, S. J. 2010. Family history of alcoholism mediates
797 the frontal response to alcoholic drink odors and alcohol in at-risk drinkers.
798 *Neuroimage,* 50**,** 267-76.

KEISTLER, C. R., HAMMARLUND, E., BARKER, J. M., BOND, C. W., DILEONE, R. J., PITTENGER, C. & TAYLOR, J. R. 2017. Regulation of alcohol extinction and cue-induced reinstatement by specific projections between medial prefrontal cortex, nucleus accumbens and basolateral amygdala. *J Neurosci*.

KRAWCZYK, D. C. 2002. Contributions of the prefrontal cortex to the neural basis of human decision making. *Neurosci Biobehav Rev,* 26**,** 631-64.

LI, T. K. & MCBRIDE, W. J. 1995. Pharmacogenetic models of alcoholism. *Clin Neurosci,* 3**,** 182-8.

LINSENBARDT, D. N. & LAPISH, C. C. 2015. Neural Firing in the Prefrontal Cortex During Alcohol Intake in Alcohol-Preferring "P" Versus Wistar Rats. *Alcohol Clin Exp Res,* 39**,** 1642-53.

LUMENG, L. & LI, T. K. 1986. The development of metabolic tolerance in the alcohol-preferring P rats: comparison of forced and free-choice drinking of ethanol. *Pharmacol Biochem Behav,* 25**,** 1013-20.

MCBRIDE, W. J. & LI, T. K. 1998. Animal models of alcoholism: neurobiology of high alcohol-drinking behavior in rodents. *Crit Rev Neurobiol,* 12**,** 339-69.

MCBRIDE, W. J., RODD, Z. A., BELL, R. L., LUMENG, L. & LI, T. K. 2014. The alcohol-preferring (P) and high-alcohol-drinking (HAD) rats--animal models of alcoholism. *Alcohol,* 48**,** 209-15.

MCCANE, A. M., CZACHOWSKI, C. L. & LAPISH, C. C. 2014. Tolcapone suppresses ethanol intake in alcohol-preferring rats performing a novel cued access protocol. *Alcohol Clin Exp Res,* 38**,** 2468-78.

MOMENNEJAD, I. & HAYNES, J. D. 2013. Encoding of prospective tasks in the human prefrontal cortex under varying task loads. *J Neurosci,* 33**,** 17342-9.

MYRICK, H., ANTON, R. F., LI, X., HENDERSON, S., DROBES, D., VORONIN, K. & GEORGE, M. S. 2004. Differential brain activity in alcoholics and social drinkers to alcohol cues: relationship to craving. *Neuropsychopharmacology,* 29**,** 393-402.

PANZERI, S., SENATORE, R., MONTEMURRO, M. A. & PETERSEN, R. S. 2007. Correcting for the sampling bias problem in spike train information measures. *J Neurophysiol,* 98**,** 1064-72.

PFARR, S., MEINHARDT, M. W., KLEE, M. L., HANSSON, A. C., VENGELIENE, V., SCHONIG, K., BARTSCH, D., HOPE, B. T., SPANAGEL, R. & SOMMER, W. H. 2015. Losing Control: Excessive Alcohol Seeking after Selective Inactivation of Cue-Responsive Neurons in the Infralimbic Cortex. *J Neurosci,* 35**,** 10750-61.

RANGEL, A., CAMERER, C. & MONTAGUE, P. R. 2008. A framework for studying the neurobiology of value-based decision making. *Nat Rev Neurosci,* 9**,** 545-56.

REDISH, A. D., JENSEN, S. & JOHNSON, A. 2008. A unified framework for addiction: vulnerabilities in the decision process. *Behav Brain Sci,* 31**,** 415-37; discussion 437-87.

RIDDERINKHOF, K. R., VAN DEN WILDENBERG, W. P., SEGALOWITZ, S. J. & CARTER, C. S. 2004. Neurocognitive mechanisms of cognitive control: the role of prefrontal cortex in action selection, response inhibition, performance monitoring, and reward-based learning. *Brain Cogn,* 56**,** 129-40.

ROXIN, A., BRUNEL, N., HANSEL, D., MONGILLO, G. & VAN VREESWIJK, C. 2011. On the distribution of firing rates in networks of cortical neurons. *J Neurosci,* 31**,** 16217-26.

SAKAGAMI, M. & NIKI, H. 1994. Encoding of behavioral significance of visual stimuli by primate prefrontal neurons: relation to relevant task conditions. *Exp Brain Res,* 97**,** 423-36.

SAKAGAMI, M. & TSUTSUI, K. 1999. The hierarchical organization of decision making in the primate prefrontal cortex. *Neurosci Res,* 34**,** 79-89.

SCHACHT, J. P., ANTON, R. F. & MYRICK, H. 2013. Functional neuroimaging studies of alcohol cue reactivity: a quantitative meta-analysis and systematic review. *Addict Biol,* 18**,** 121-33.

SEIF, T., CHANG, S. J., SIMMS, J. A., GIBB, S. L., DADGAR, J., CHEN, B. T., HARVEY, B. K., RON, D., MESSING, R. O., BONCI, A. & HOPF, F. W. 2013. Cortical activation of accumbens hyperpolarization-active NMDARs mediates aversion-resistant alcohol intake. *Nat Neurosci,* 16**,** 1094-100.

SEIF, T., SIMMS, J. A., LEI, K., WEGNER, S., BONCI, A., MESSING, R. O. & HOPF, F. W. 2015. D-Serine and D-Cycloserine Reduce Compulsive Alcohol Intake in Rats. *Neuropsychopharmacology,* 40**,** 2357-67.

SIMMS, J. A., STEENSLAND, P., MEDINA, B., ABERNATHY, K. E., CHANDLER, L. J., WISE, R. & BARTLETT, S. E. 2008. Intermittent access to 20% ethanol induces high ethanol consumption in Long-Evans and Wistar rats. *Alcohol Clin Exp Res,* 32**,** 1816-23.

STEWART, R. B., MCBRIDE, W. J., LUMENG, L., LI, T. K. & MURPHY, J. M. 1991. Chronic alcohol consumption in alcohol-preferring P rats attenuates subsequent conditioned taste aversion produced by ethanol injections. *Psychopharmacology (Berl),* 105**,** 530-4.

TANJI, J. & HOSHI, E. 2001. Behavioral planning in the prefrontal cortex. *Curr Opin Neurobiol,* 11**,** 164-70.

TAPERT, S. F., CHEUNG, E. H., BROWN, G. G., FRANK, L. R., PAULUS, M. P., SCHWEINSBURG, A. D., MELOY, M. J. & BROWN, S. A. 2003. Neural response to alcohol stimuli in adolescents with alcohol use disorder. *Arch Gen Psychiatry,* 60**,** 727-35.

TIMME, N. M. & LAPISH, C. 2018. A Tutorial for Information Theory in Neuroscience. *eNeuro,* 5.

TIMME, N. M., MARSHALL, N. J., BENNETT, N., RIPP, M., LAUTZENHISER, E. & BEGGS, J. M. 2016. Criticality Maximizes Complexity in Neural Tissue. *Front Physiol,* 7**,** 425.

TREVES, A. & PANZERI, S. 1995. The upward bias in measures of information derived from limited data samples. *Neural Comput.,* 7**,** 399-407.

VERDEJO-GARCIA, A., CHONG, T. T., STOUT, J. C., YUCEL, M. & LONDON, E. D. 2017. Stages of dysfunctional decision-making in addiction. *Pharmacol Biochem Behav*.

WALLER, M. B., MCBRIDE, W. J., LUMENG, L. & LI, T. K. 1982. Induction of dependence on ethanol by free-choice drinking in alcohol-preferring rats. *Pharmacol Biochem Behav,* 16**,** 501-7.

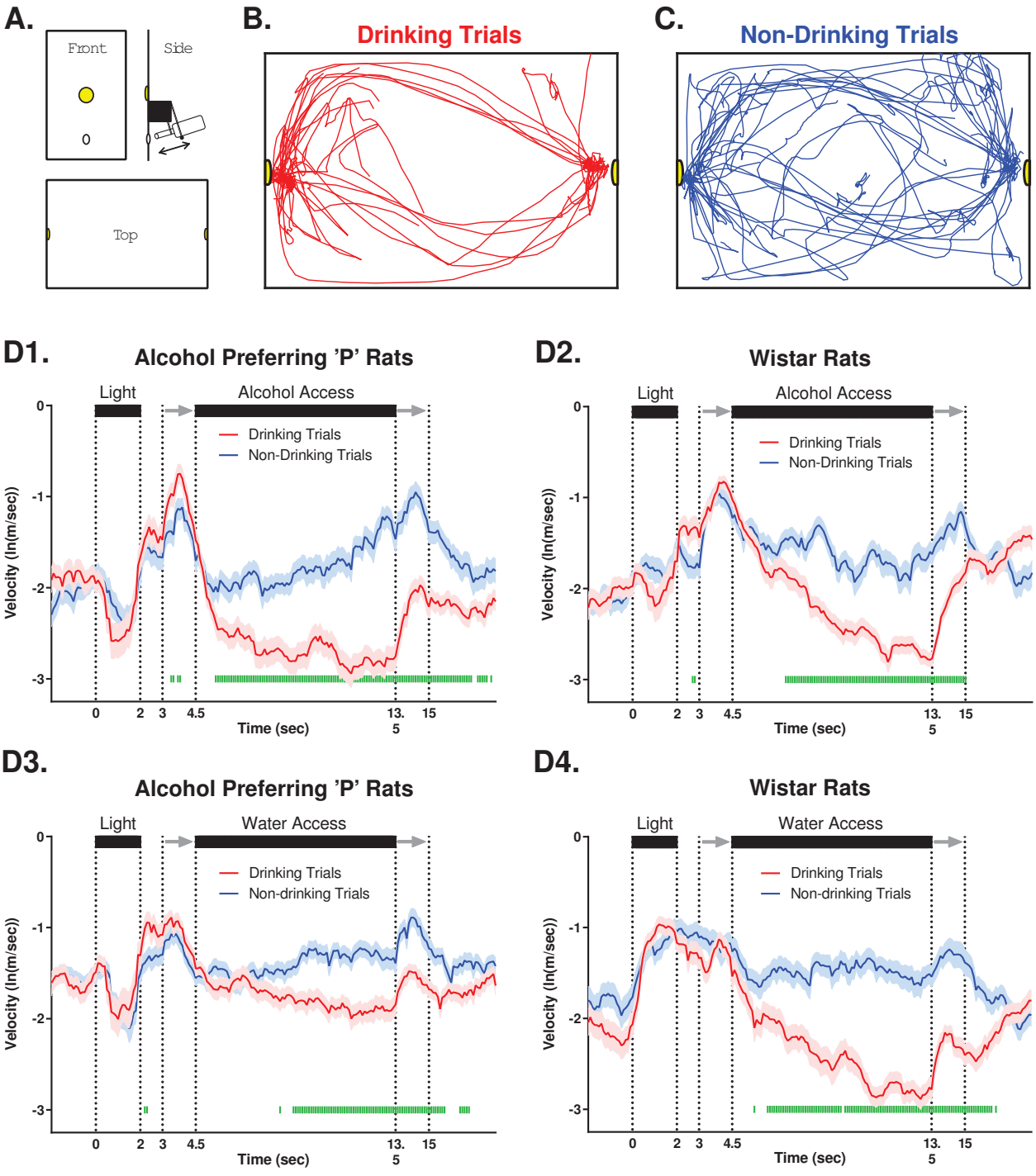

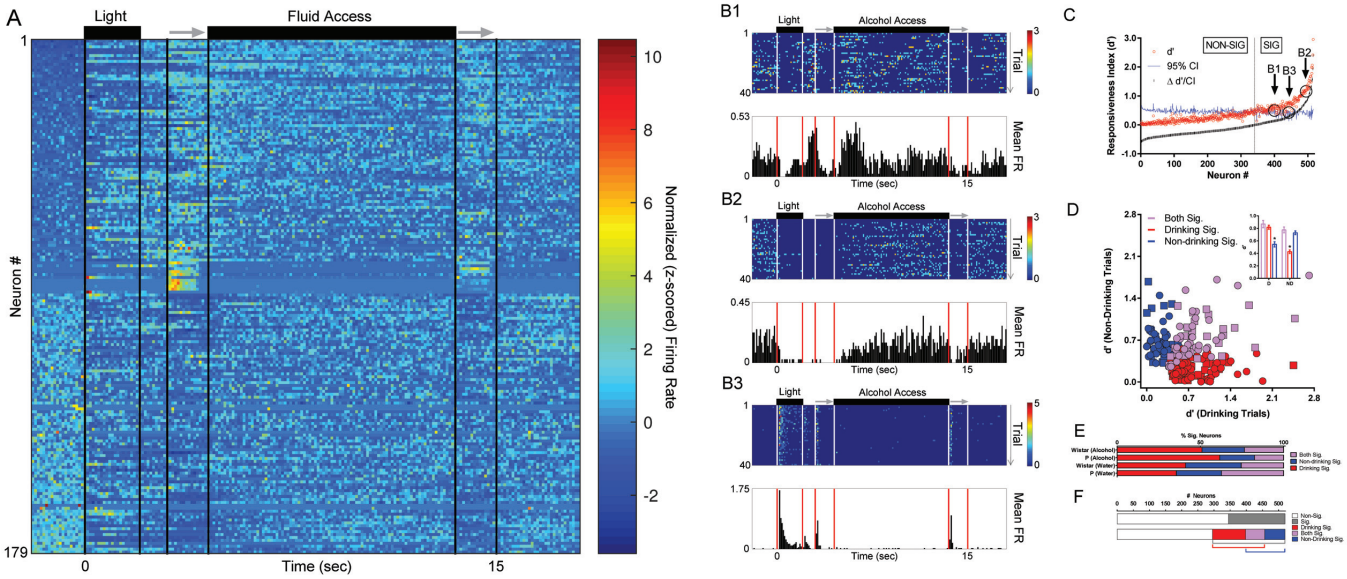

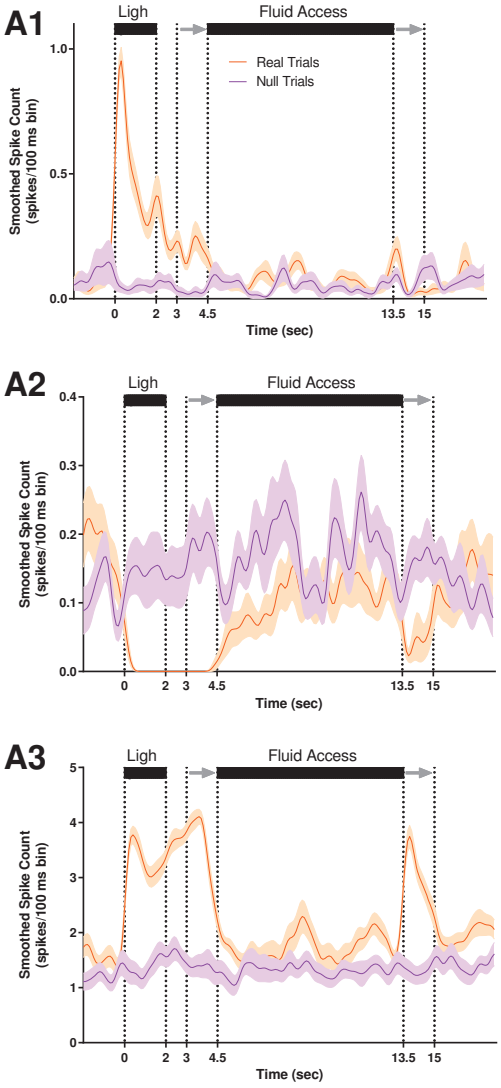

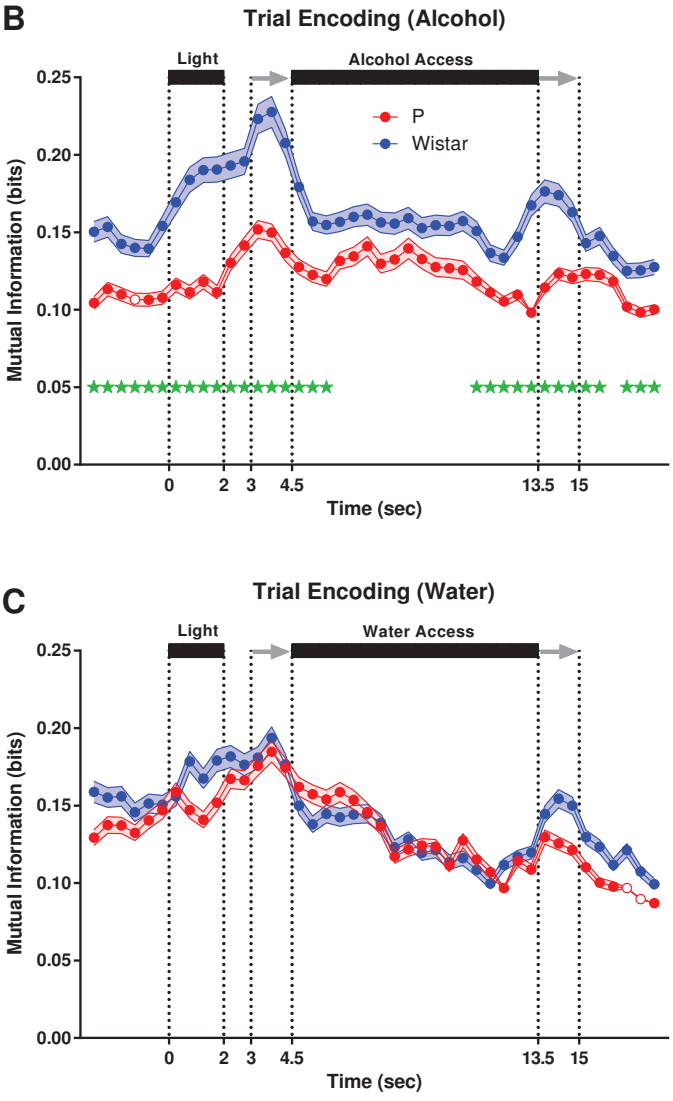

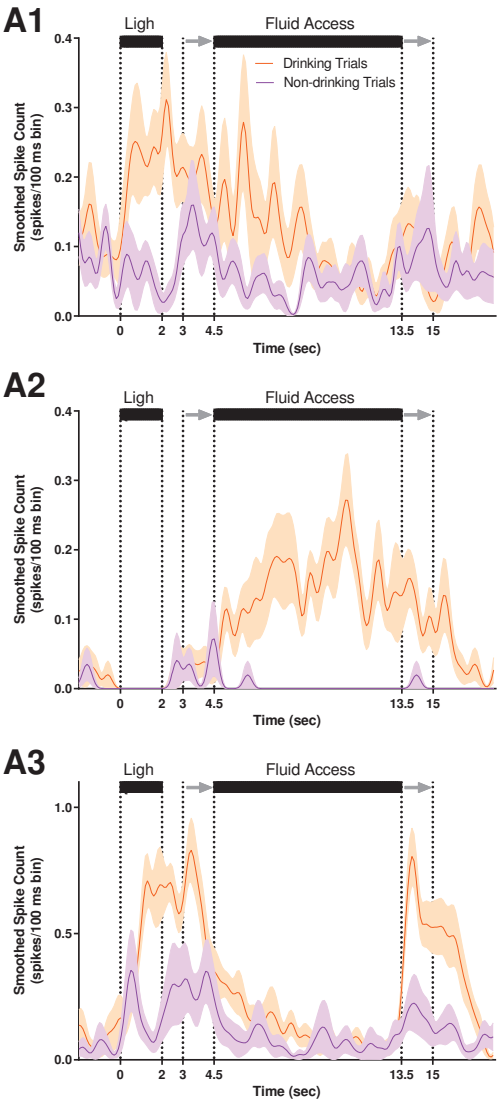

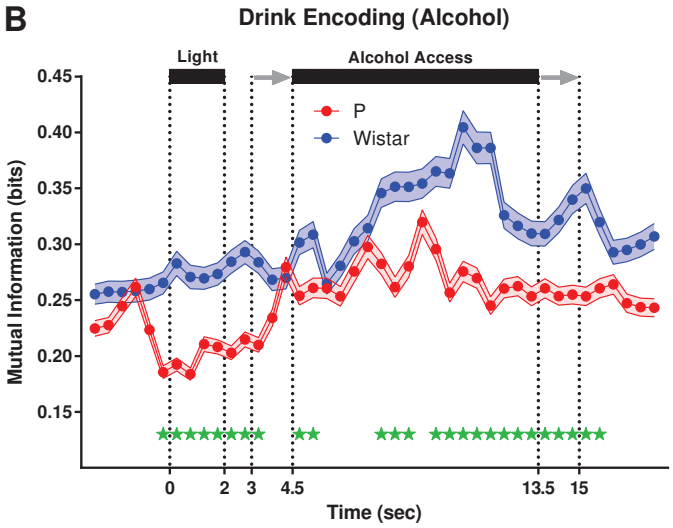

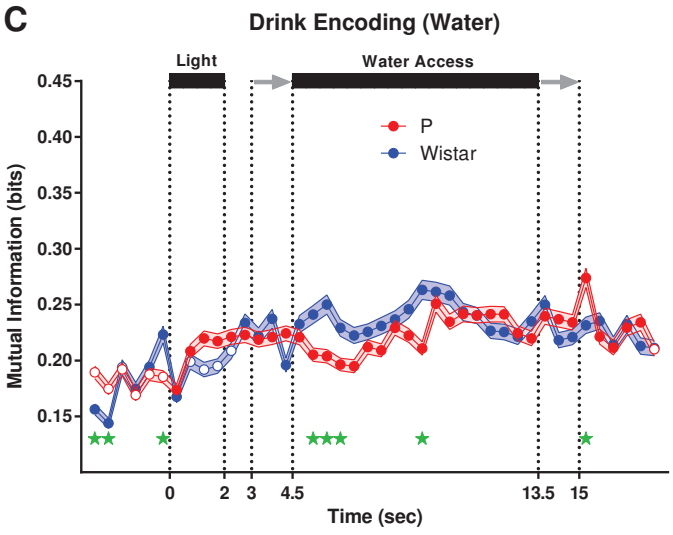

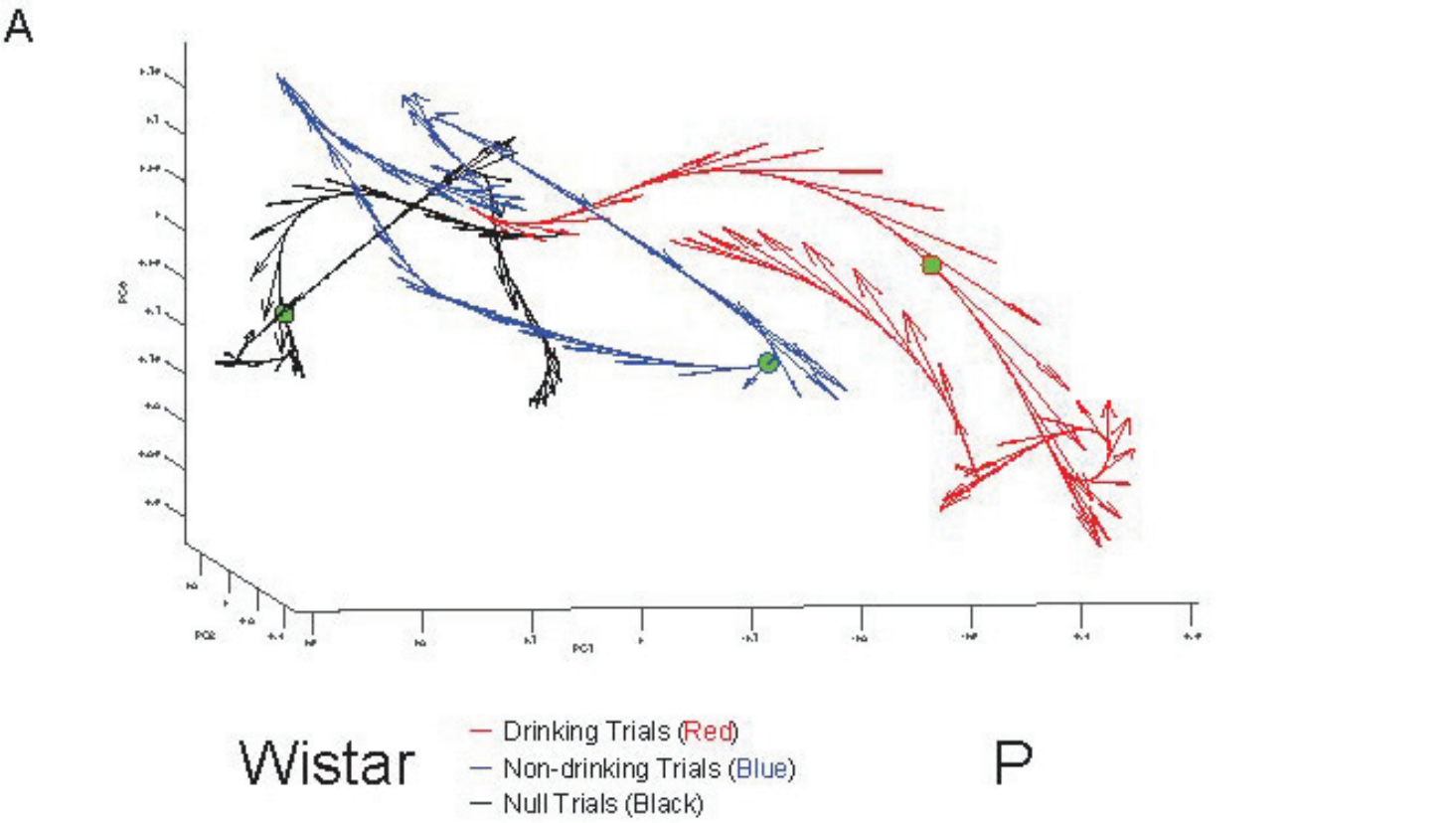

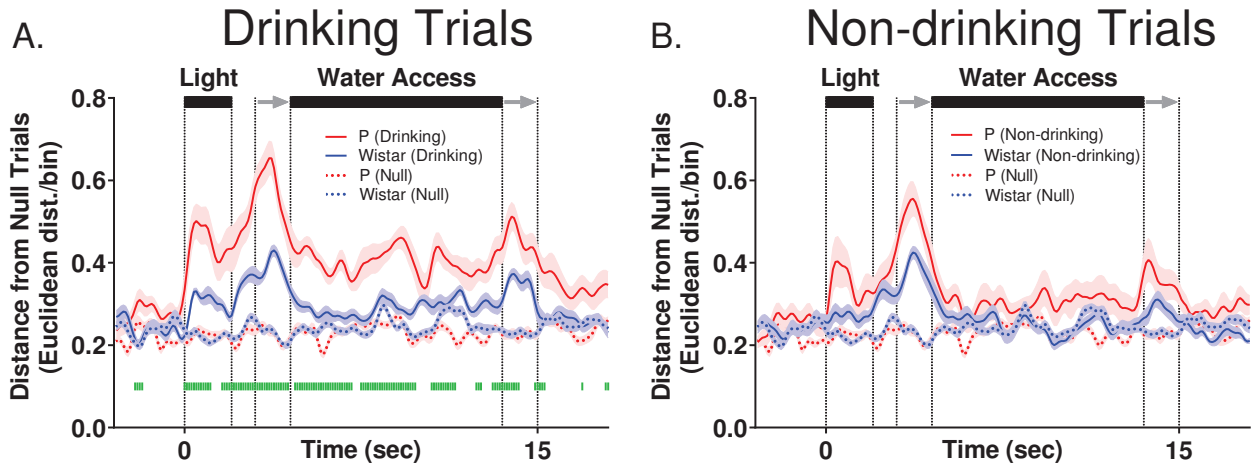

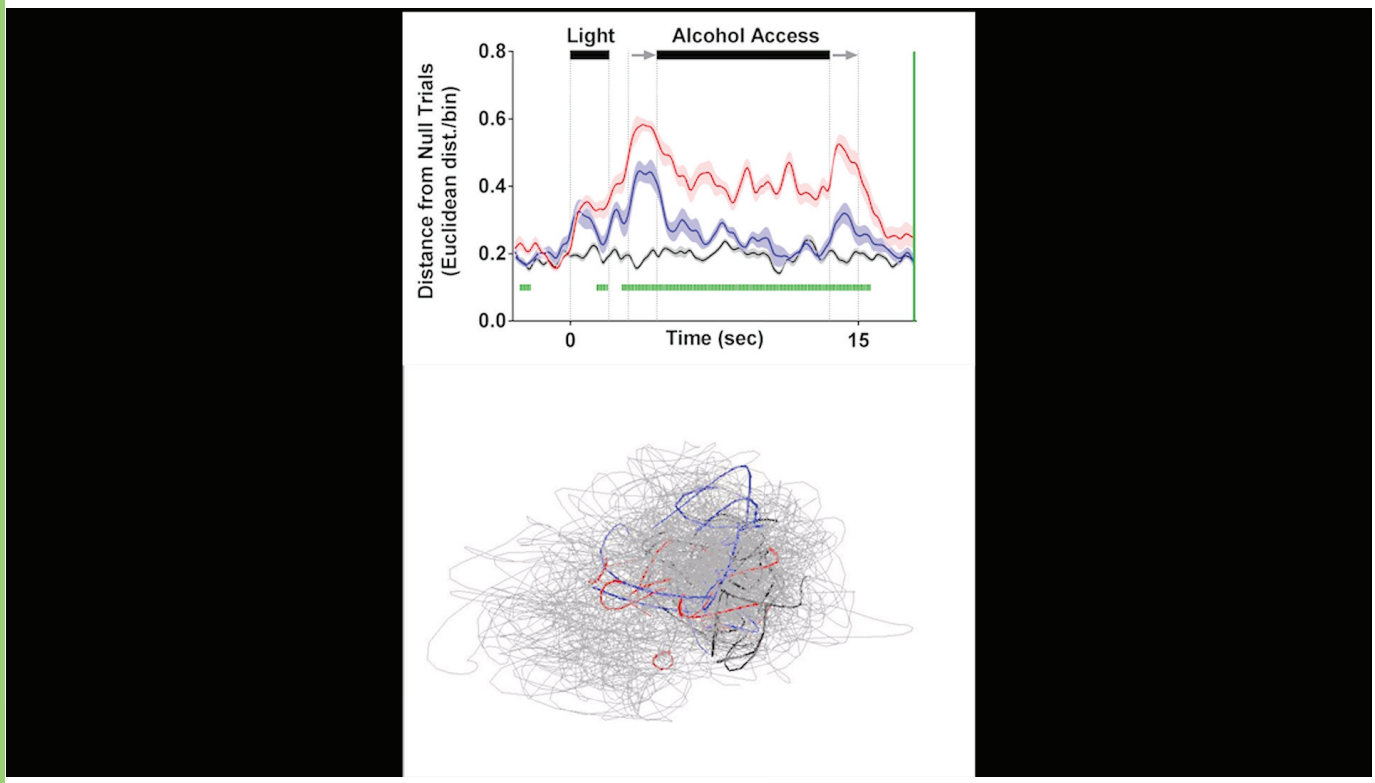

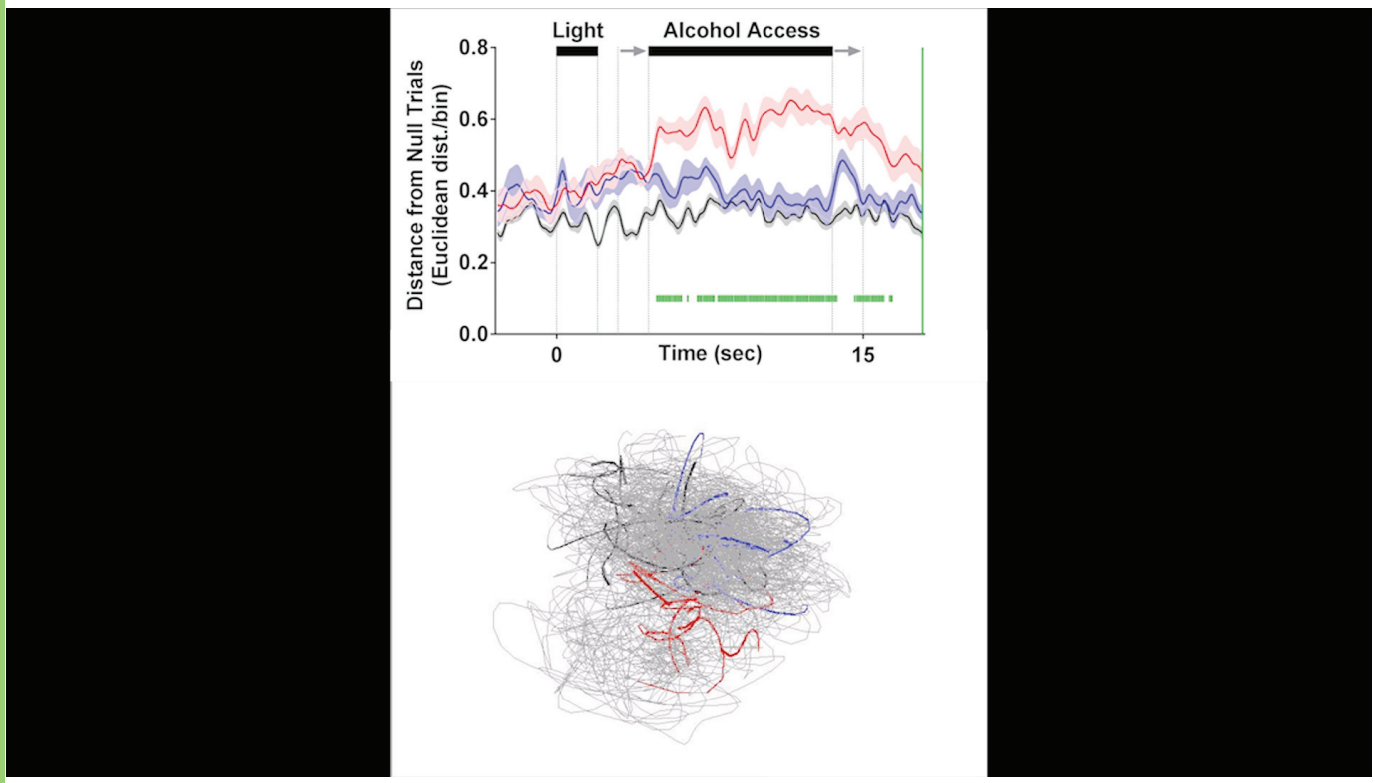

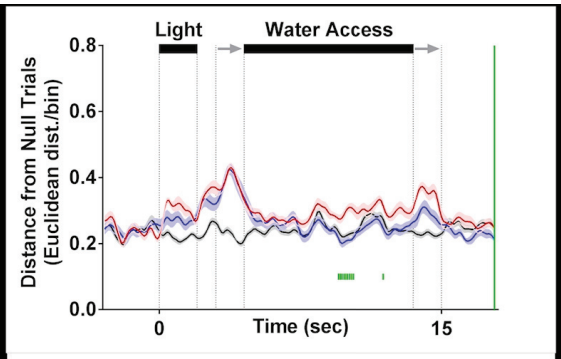

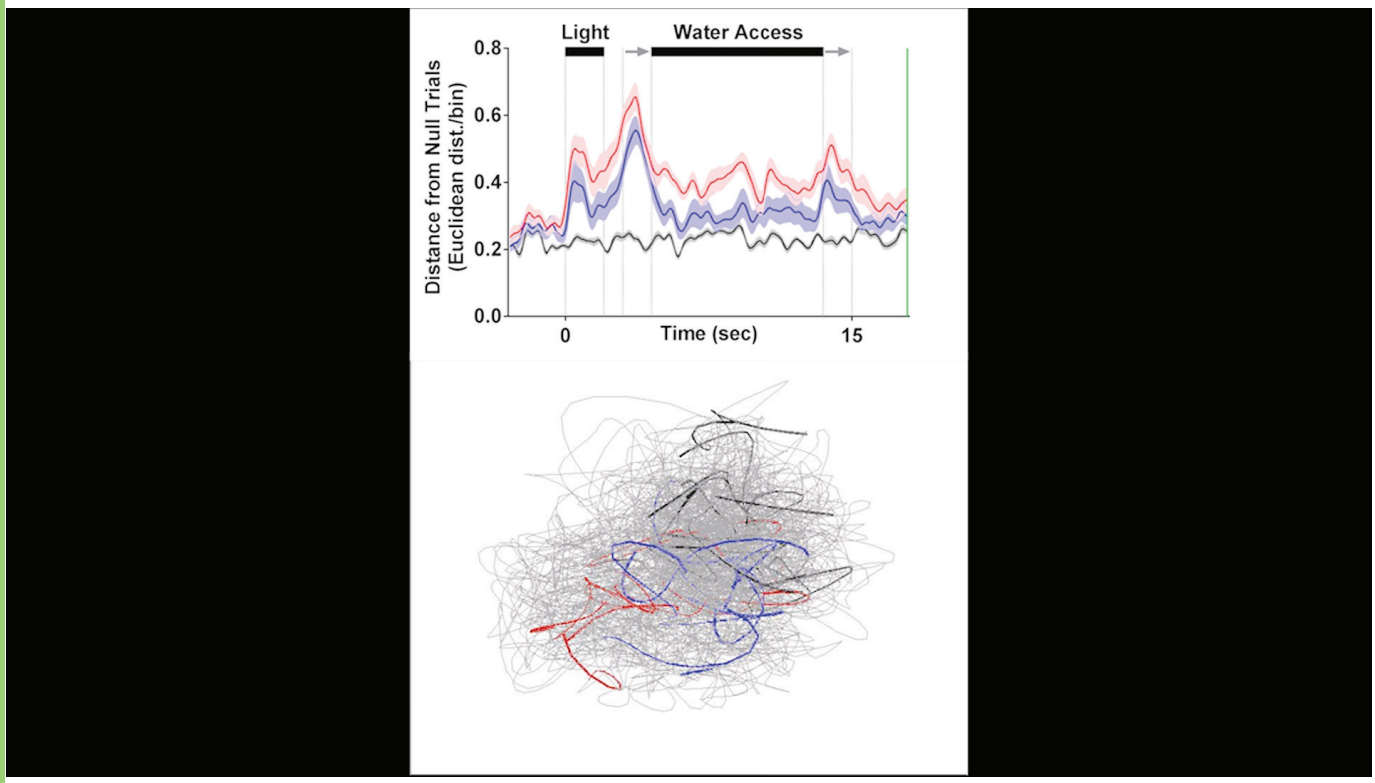

Table 1. Detailed statistics summary

	Figure	Comparison	Data structure	Type of test	Statistic	Confidence, 95% CI
a	1D1-4	Drinking vs. Non-drinking Movement	Non-normal	FDR-corrected rank-sum		p<0.05
b	2C	Neuron Responsivenes	Normal	d' (d-prime)		p<0.05
c	2D inset	Neuron Responsivenes (Drinking vs. Non-drinking)	Normal	2-way ANOVA	Df=2; F=38.03	p<0.0001
d	2E	Neuron Responsiveness Proportions: Alcohol	Normal	χ2 (Chi-squared)	χ2=3.24	p=0.20
e	2E	Neuron Responsiveness Proportions: Water	Normal	χ2 (Chi-squared)	χ2=2.34	p=0.31
f	3B+C	Trial Encoding	Non-Normal	FDR-corrected rank-sum		p<0.05
g	4B+C	Drink Encoding	Non-Normal	FDR-corrected rank-sum		p<0.05
h	5B-E	Neural Population State-Space	Non-Normal	FDR-corrected rank-sum		p<0.05
i	6	Neural Population State-Space	Non-Normal	FDR-corrected rank-sum		p<0.05